2 FACTOR-OF-SAFETY CALCULATION

2.1 Introduction

This section describes the factor-of-safety calculation that can be used for stability analyses in *UDEC*. This calculation is based upon the "strength reduction method" to determine a factor of safety. The strength reduction method is an increasingly popular numerical method to evaluate factor of safety in geomechanics (e.g., see Dawson and Roth 1999, and Griffiths and Lane 1999). Although the method has been used extensively in the context of Mohr-Coulomb material, there are a few references available in the literature that extend the approach to nonlinear failure criteria in general (e.g., Dawson et al. 2000, Shukha and Baker 2003, Hammah et al. 2005, and Fu and Liao 2009). An overview of factor of safety and the strength reduction technique is given in Section 2.2.

The strength reduction method can be applied to calculate the safety factor for a variety of different underground structures (e.g., slopes, retaining walls, tunnels, etc.). In this section, the focus is on the factor of safety of slopes because this is the most common practical application of the method. The strength reduction method is described and compared to other computational methods commonly used to determine a safety factor for slopes in Section 2.3.

The strength reduction procedure can be conducted manually in *UDEC* by reducing selected strength properties until failure occurs. The method can also be performed automatically by issuing the **block factor-of-safety** command in *UDEC*. The procedure that is followed when using **block factor-of-safety** is described in detail in Section 2.4. In *UDEC* Version 7.0, **block factor-of-safety** can be applied to strength properties for the Mohr-Coulomb material model (**block zone cmodel assign mohr**), the ubiquitous-joint model **block zone cmodel assign ubiquitous**) and the Hoek-Brown model (**block zone cmodel assign hoek-brown**). It also can be applied to strength properties for joints using the Coulomb joint model (**block contact cmodel assign area**), and to selected strength properties for structural elements. The properties affected by **block factor-of-safety** are described in Section 2.4.1.

Example factor-of-safety calculations are also provided in this section. These are described and data files are listed in Section 2.5.

2.2 Factor of Safety

A "factor of safety" index can be defined for any relevant problem parameter by taking the ratio of the calculated parameter value under given conditions to the critical value of the parameter, at which the onset of an unacceptable outcome manifests itself. A relevant problem parameter could be a dimensionless group that governs the problem at hand (e.g., a stability number). Examples of (dimensional) parameters for slope stability include slope height, water level, applied load and strength property.

Unacceptable outcome relates to "safety" (and is usually taken as shear failure), but other possibilities, such as displacement above a given threshold, convergence beyond an acceptable level (such as in a tunnel excavation), toppling failure, slope raveling (cyclic freezing/thawing, weathering), etc., can also be considered.

By convention, a factor-of-safety index larger than one indicates acceptable conditions. Thus, factor-of-safety index is taken as the actual over the critical parameter value if the parameter value above critical is acceptable (e.g., material cohesion), and as the inverse of this ratio otherwise (e.g., slope height). Note that, with the exception of simple cases, the calculated factor-of-safety index will not (in general) be linearly related to the selected problem parameter for which it is defined. Also, different measures will give different values of factor of safety for the same problem. Factor-of-safety index is most valuable when used on a comparative basis, in analyses using the same index definition (e.g., use of the index may produce the following statement: this slope with wider benches has a higher index than that with higher benches).

The effort involved in computing the factor-of-safety index (once the definition is established) consists of identifying actual as well as critical parameter values. In the most general case, the actual parameter value is evaluated by direct resolution of field and constitutive equations governing the problem, and this often is being done using a numerical method. On the other hand, an inverse boundary value problem needs to be solved to estimate the critical value of the parameter. In principle, this can be achieved using a trial-and-error technique whereby numerical simulations are performed for a range of parameter values until the critical value is found. We refer to this general approach as "parameter reduction technique." Any appropriate geomechanical software (e.g., finite difference, finite element and distinct element method) can be used to perform this task for problems involving various levels of complexity (e.g., geometry, material constitutive law, discrete fracture network, slope reinforcement, support systems, mechanical structures, etc.).

2.3 Computational Methods to Calculate the Factor of Safety of Slopes

Three different computational methods are commonly employed in numerical analyses programs to calculate a factor of safety for slopes: strength reduction method, limit analysis (upper- and lower-bound solutions), and limit equilibrium method (upper-bound solution). The strength reduction method is used in *UDEC*, and can be executed automatically via the **block factor-of-safety** command. This implementation is described below. Numerical limit analysis is described in Section 2.3.2, and limit equilibrium analysis is described in Section 2.3.3.

2.3.1 Strength Reduction Technique

The "strength reduction technique" is typically applied in factor-of-safety calculations by progressively reducing the shear strength of the material to bring the slope to a state of limiting equilibrium. The method is commonly applied with the Mohr-Coulomb failure criterion (e.g., see applications by Zienkiewicz et al. 1975, Naylor 1982, Donald and Giam 1988, Matsui and San 1992, Ugai 1989, and Ugai and Leshchinsky 1995). In this case, the safety factor F is defined according to the equations

$$c^{\text{trial}} = \frac{1}{F^{\text{trial}}}\, c \tag{2.1}$$

$$\phi^{\text{trial}} = \arctan\left(\frac{1}{F^{\text{trial}}} \tan\phi\right) \tag{2.2}$$

A series of simulations are made using trial values of the factor F^{trial} to reduce the cohesion, c, and friction angle, ϕ, until slope failure occurs. (Note that if the slope is initially unstable, c and ϕ will be *increased* until the limiting condition is found.) One technique to find the strength values that correspond to the onset of failure is to monotonically reduce (or increase) the strengths in small increments until a failure state is found. Alternatively, in *UDEC*, a bracketing approach similar to that proposed by Dawson, Roth and Drescher (1999) is used when the **block factor-of-safety** command is executed. With this technique, stable and unstable bracketing states are found first, and then the bracket between the stable and unstable solution is progressively reduced until the difference between stable and unstable solutions falls below a specified tolerance.

The strength reduction method implemented in *UDEC* will always produce a valid solution: in the case of an unstable physical system, *UDEC* simply shows continuing motion in the model. An iteration solution, which is often used in the finite element method, is not used here. The *UDEC* solution is a dynamic, time-marching simulation in which continuing motion is as valid as equilibrium. Neither is there iteration in the use of elastic-plastic constitutive laws: the stress tensor is placed exactly on the yield surface (satisfying equations such as the flow rule and elastic/plastic strain decomposition) if plastic yield is detected. The stress state in *UDEC* at a safety factor = 1 is the actual stress state that corresponds to the yielding mechanism, not an arbitrary pre-yield stress state or an elastic stress state.

The detection of the boundary between physical stability and instability is based on an objective criterion in *UDEC* that determines whether the system is in equilibrium or a state of continuing motion. Finer incremental changes that may affect the solution in an iterative solution scheme are not needed in a time-marching scheme, and do not affect the solution. In order to determine the boundary between physical stability and instability, a set of completely separate runs is made with different strength-reduction factors. Each run is then checked to determine whether equilibrium or continuing plastic flow is reached. The point of failure can be found to any required accuracy (typically 1%) by successive bracketing of the strength-reduction factors. This process should not be confused with taking finer solution steps; the solution scheme is *identical* for each run of the set (whether it results in equilibrium or continuing motion).

2.3.2 Limit Analysis

Limit analysis relies on the construction of solutions that obey upper- and lower-bound theorems developed in the theory of plasticity. These theorems (presented in most textbooks on plasticity) provide rigorous limits on the collapse conditions of a system consisting of a perfectly plastic material obeying normality (associated flow rule). Of particular interest is the lower-bound theorem, which states (Davis and Selvadurai 2002) that

Collapse will not occur if any state of stress can be found that satisfies the equations of equilibrium and the traction boundary conditions and is everywhere 'below yield'.

In this theorem, the words "equations of equilibrium" pertain to local equilibrium. Any stress field that satisfies the criteria of the lower-bound theorem is referred to as a statically admissible stress field. Also, in a factor-of-safety calculation, a statically admissible stress field provides a lower-bound (conservative) estimate for the FOS.

It is also useful to recall the upper-bound theorem, which states that (Davis and Selvadurai 2002)

Collapse must occur if, for any compatible plastic deformation, the rate of working of the external forces on the body equals or exceeds the rate of internal energy dissipation.

In this statement, "compatible plastic deformation" means any deformation that satisfies all displacement boundary conditions and is possible kinematically according to the associated flow rule, which governs admissible dilation. Any deformation field that satisfies the criteria of the upper-bound theorem is referred to as kinematically admissible deformation.

Stability charts for homogeneous simple slope (in "cohesive" material) are still used in practice as a first estimate of slope safety. Typically, values in the chart obtained using limit analysis (upper- and lower-bound solutions) are presented in the form of stability numbers (see, e.g., Taylor 1937, Dawson et al. 2000, Michalowski 2002, and Li et al. 2008). These numbers are dimensionless quantities that relate slope height, material unit weight, and the material strength property of cohesion for a Mohr-Coulomb material, or intact unconfined compressive strength for a Hoek-Brown material. Stability numbers have been associated with nontraditional FOS measures – e.g., for Mohr-Coulomb (Michalowski 2002) and for Hoek-Brown (Li et al. 2008).

2.3.3 Limit Equilibrium

Limit equilibrium (LE) methods are approximate methods that assume the existence of a slip surface of various simple shapes: plane, circular or logspiral. The methods are based on the additional assumption that the soil or rock mass can be divided into slices. The problem is reduced to one of finding the most critical position for the slip surface of the chosen shape. Various methods exist, including Fellenius' (1936), Bishop's (1955), Lowe and Karafiath's (1960), Janbu's (1968), Morgenstern and Price's (1965) and Spencer's (1967). One of the main differences between methods concerns assumptions made about side force directions between slices, with potential implications for equilibrium. A comparative description summary of methods with assumptions and limitations may be found in TRB Special Report (1996) and Abramson et al. (2002).

Note that none of the equations of solid mechanics is explicitly satisfied inside or outside the failure surface (assumed slip surface). Also, according to Chen (2007):

Although the limit equilibrium technique utilizes the basic philosophy of the upper-bound rules of limit analysis, that is, a failure surface is assumed and a least answer is sought, it does not meet the precise requirements of the upper-bound rules so that it is not an upper bound. The method basically gives no consideration to soil kinematics, and equilibrium conditions are satisfied only in a limited sense. It is clear then that a solution obtained using the limit equilibrium method is not necessarily an upper or a lower bound.

2.3.4 Relation of Strength Reduction Method to Limit Equilibrium and Limit Analysis

As mentioned in Section 2.3.3, a limit equilibrium (LE) solution is never a lower bound for the load because, although global equilibrium is satisfied by the LE solution, local equilibrium is not guaranteed (none of the LE solutions are statically admissible).

Also, a strong statement made in the literature (e.g., Davis and Selvadurai 2002) is that the results from LE will always be the same as those from the upper-bound theorem for any translational collapse mechanism (meaning a system of rigid soil blocks separated by thin shear surfaces). Thus, there are cases for which an LE solution gives an upper bound for the load (Drescher and Detournay 1993).

One may ask then why an LE solution "works" since not only is it not guaranteed to provide a lower bound for the FOS, but in some cases it is even proven to give an upper bound for the FOS. An answer, provided by Wa-I-Fah Chen in his book ***Limit Analysis and Soil Plasticity***, rests on the observation that most FOS analyses are concerned with slopes, and apparently, for most slopes, the LE solution provides an FOS value close to the exact solution.

On the other hand, consider the last stable state calculated by *UDEC* (the last lower bracket, which is typically 0.005 less than the final FOS) for an associated problem. *UDEC* will provide an approximate exact solution to the problem at that state, in the sense that local equilibrium may not be satisfied everywhere at the boundary between zones, but if the zone size is reduced to zero, local equilibrium will be satisfied to the limit. In particular, the limit stress field satisfies the lower-bound theorem. Also, the deformation field at the "failure state" calculated by *UDEC* (the last upper bracket) is a kinematically admissible deformation (it fulfills all the criteria of the upper-bound

theorem). Thus one may say that if the calculated FOS tends to a limit as the grid size is reduced, this limit may be considered to be very close to (within 0.005) the exact FOS for the problem.

In summary, in most cases *UDEC* (on a fine grid) and an LE solution will give factors of safety that are very similar. In some cases *UDEC* will give a safety factor on a fine grid that is lower than that provided by a limit equilibrium (LE) solution. This implies that the LE solution provides an upper bound for the FOS. In other cases *UDEC* will give a safety factor on a fine grid that is higher than that provided by a limit equilibrium (LE) solution. This does not mean that *UDEC* is nonconservative, but instead that we have encountered a case where the LE solution cannot be relied upon (since it can never correspond to a lower bound for the load).

Note that the limit-analysis bound theorems apply to an associated flow rule (see Davis and Selvadurai 2002). This rule may not be very realistic in some cases, as it provides far too much dilation. However, nonassociated flow rules do not guarantee unique solutions. Without this assurance, a collapse load is no longer unique. Apparently, the only useful result that can be obtained is that a nonassociative material can be no stronger than an associative one. This follows from the observation that, at collapse, the actual stress field in a nonassociative soil is statically admissible. Therefore, by the lower-bound theorem, the collapse load for a nonassociative material cannot exceed that for the corresponding material with the associated flow rule.

2.4 Strength Reduction Procedure in *UDEC*

The strength reduction method can be applied to essentially any material failure model to evaluate a factor of safety based upon the reduction of a specified strength property or property group. The method has been used extensively in the context of Mohr-Coulomb material and, principally, the simultaneous reduction of cohesion and frictional strength. In *UDEC* Version 6.0, in addition to Mohr-Coulomb strength properties (assigned with **block zone cmodel assign mohr**), the method is also applied automatically to ubiquitous-joint strength properties (assigned with **block zone cmodel assign ubiquitous**), and to Hoek-Brown strength properties (assigned with **block zone cmodel assign hoek-brown**) when the **block factor-of-safety** command is given for models with deformable blocks.

The strength reduction method is also applied automatically when **block factor-of-safety** is given for joint strength properties when using Coulomb joints (assigned via **block contact cmodel assign area**). If structural elements are included in a *UDEC* model, the method is automatically applied to grout shear strength and axial yield strengths of cables, axial and shear load limits for local reinforcement, axial yield strengths of liners, and axial compressive loads of supports when **block factor-of-safety** is issued.

The procedure for implementing the strength reduction technique in *UDEC* via the **block factor-of-safety** command is as follows.

First, the code finds a "characteristic response time," which is a representative number of steps (denoted by N_r) that characterizes the response time of the system. N_r is found by setting the material strength (for Mohr-Coulomb material, the cohesion and tensile strength) to a large value, making a large change to the internal stresses (by default, a perturbation factor of 2 is applied to the stress state), and finding how many steps are necessary for the system to return to equilibrium.

A maximum limit of 50,000 is set for N_r by default. If the model does not reach equilibrium within 50,000 steps, the run will stop, and the factor-of-safety solution cannot be completed. If this happens, the user should review the parameters selected for the model. For example, if the user has selected structural support with a high value for Young's modulus, this may affect the solution convergence time. If N_r is not found within 50,000 steps, the characteristic response step limit can be changed with the optional keyword **step-limit** following the **block factor-of-safety** command.

It is also possible to set the value for N_r manually by using the **characteristic-steps** keyword to specify a value for N_r. Alternatively, the initial perturbation to the internal stresses can be changed by specifying a different perturbation factor using the **perturbation** keyword. Note that these manual controls should be used with caution.

After N_r is determined for a given strength reduction factor, F, N_r steps are executed. If the unbalanced force ratio* is less than 10^{-3} after N_r steps, then the system is in equilibrium. If the

---

* The *unbalanced force* is the net force acting on a *UDEC* gridpoint. The ratio of this force to the mean absolute value of force exerted by each surrounding zone is the *unbalanced force ratio*. The limiting value for the unbalanced force ratio can be changed with the optional keyword **ratio** to the **block factor-of-safety** command.

unbalanced force ratio is greater than 10^{-3}, then another N_r steps are executed, exiting the loop if the force ratio is less than 10^{-3}. The mean value of force ratio, averaged over the current span of N_r steps, is compared with the mean force ratio over the previous N_r steps. If the difference is less than 10%, the system is deemed to be in nonequilibrium, and the loop is exited with the new nonequilibrium, F. If the above-mentioned difference is greater than 10%, blocks of N_r steps are continued until (1) the difference is less than 10%; or (2) 6 such blocks have been executed; or (3) the force ratio is less than 10^{-3}. The justification for case (1) is that the mean force ratio is converging to a steady value that is greater than that corresponding to equilibrium; the system must therefore be in continuous motion.

The following information is displayed during the solution process.

1. Number of calculation steps completed to determine a given value of F, as a percentage of N_r.
2. Number of completed solution cycles (i.e., tests for equilibrium or nonequilibrium).
3. Operation currently being performed.
4. Current bracketing values of F.

The factor-of-safety solution stops when the difference between the upper- and lower-bracket values becomes smaller than 0.005. (This resolution limit can be changed with the optional keyword **resolution** to the **block factor-of-safety** command.)

The bracketing solution approach invoked with the **block factor-of-safety** command may perform a large number of (stable and unstable) solutions before determining a factor of safety. If an approximate range for the factor is known, then the number of solutions (and total solution time) can be reduced by specifying the starting bracket values. This can be done with the optional phrase **bracket *v1 v2*** to the **block factor-of-safety** command. If the calculated factor falls outside the specified brackets, a warning message will be issued. It is also possible to test whether a specified factor is above or below the actual factor, by setting ***v1*** equal to ***v2***.

The following conditions should be noted when using **block factor-of-safety**.

1. The model state must be saved before a **block factor-of-safety** calculation is performed.
2. The initial stress state can either be at a zero stress state or stress equilibrium for the **block factor-of-safety** calculation. If the model is at a zero stress state, only gravity loading is applied to determine N_r.
3. The factor-of-safety calculation is performed in small-strain calculation mode when **block factor-of-safety** is issued.
4. The factor-of-safety calculation assumes nonassociated plastic flow with **block factor-of-safety**. The keyword **associated** can be added for an associated plastic flow calculation.
5. When the **block factor-of-safety** calculation is complete, the original model state is restored. The **no_restore** keyword can be given with the **block factor-of-safety** command in order to plot the failed state immediately after the calculation is complete.

2.4.1 Strength Reduction Properties

The strength properties that can be reduced when using **block factor-of-safety** are described in the following sections.

2.4.1.1 Mohr-Coulomb Material

If the Mohr-Coulomb failure criterion is prescribed for a deformable block, cohesion, c, and friction angle, ϕ, are selected, by default, to be included in the safety-factor calculation when executing **block factor-of-safety**. The reduction equations for these properties are

$$c^{\text{trial}} = \frac{1}{F^{\text{trial}}}\, c \tag{2.3}$$

$$\phi^{\text{trial}} = \arctan\left(\frac{1}{F^{\text{trial}}} \tan\phi\right) \tag{2.4}$$

with the reduction following the procedure described in Section 2.4. These strengths can optionally be excluded from the **block factor-of-safety** calculation with the keyword phrase **zone exclude cohesion** or **zone exclude friction**.

Tensile strength, σ^t, can also be included with the optional keyword phrase **zone include tension**. The trial properties for tensile strength are calculated in a manner similar to that used for material friction and cohesion. The reduction equation for the tensile strength is

$$\sigma^{t(trial)} = \frac{1}{F^{trial}}\, \sigma^t \tag{2.5}$$

2.4.1.2 Ubiquitous-Joint Material

If the ubiquitous-joint strength model is used, strength values for the intact material, c and ϕ, and strength values for the ubiquitous joints, c_j and ϕ_j, are included by default in the **block factor-of-safety** calculation. Tensile strengths, σ^t and σ_j^t, can also be selected for reduction by adding the keyword phrases **zone include tension** and **zone include utension**, respectively. The reduction equations for the intact material are the same as Eqs. (2.3) through (2.5), and for the ubiquitous joints are

$$c_j^{trial} = \frac{1}{F^{trial}} c_j \tag{2.6}$$

$$\phi_j^{trial} = \arctan\left(\frac{1}{F^{trial}} \tan\phi_j\right) \tag{2.7}$$

$$\sigma_j^{t(trial)} = \frac{1}{F^{trial}} \sigma_j^t \tag{2.8}$$

Ubiquitous-joint cohesion and friction can be excluded from the safety factor calculation with **zone include ucohesion** and **zone exclude ufriction**, respectively.

2.4.1.3 Hoek-Brown Material

The Hoek-Brown constitutive model (**block zone cmodel assign hoek-brown**) supports factor-of-safety calculations with **block factor-of-safety**. Two strength-reduction property options are available: reduction with respect to shear strength (**block zone property flag-fos=0**), and reduction with respect to unconfined compressive strength (**block zone property flag-fos=1**).

Note that, although the softening/hardening capabilities of the Hoek-Brown model can be activated *before* the factor-of-safety calculation is performed, they should be disabled (by removing the table property assignment) during the strength reduction procedure because the value of the evolution parameter is then ill-defined.

FOS with respect to Shear Strength, τ

The Hoek-Brown criterion can be approximated locally by a Mohr-Coulomb criterion:

$$\tau = \sigma' \tan\phi_c + c_c \tag{2.9}$$

where apparent cohesion and friction are given in terms of the local value of σ_3 by

$$\phi_c = 2\tan^{-1}\sqrt{N_{\phi_c}} - 90^\circ \tag{2.10}$$

$$c_c = \frac{\sigma_c^{ucs}}{2\sqrt{N_{\phi_c}}} \tag{2.11}$$

where (for compressive stresses positive) if $\sigma_3 \geq 0$:

$$N_{\phi_c} = 1 + am_b\left(m_b\frac{\sigma_3}{\sigma_{ci}} + s\right)^{a-1} \tag{2.12}$$

$$\sigma_c^{ucs} = \sigma_3(1 - N_{\phi_c}) + \sigma_{ci}\left(m_b\frac{\sigma_3}{\sigma_{ci}} + s\right)^{a} \tag{2.13}$$

and, if $\sigma_3 < 0$:

$$N_{\phi_c} = 1 + am_b(s)^{a-1} \tag{2.14}$$

$$\sigma_c^{ucs} = \sigma_{ci}(s)^{a} \tag{2.15}$$

See Section 1.6.9.3 in **Constitutive Models** for the definitions of the Hoek-Brown properties.

A pragmatic approach to evaluate a factor of safety for slopes based on the strength reduction technique is used, whereby local cohesion, c_c, and friction coefficient, $\tan\phi_c$, are divided by a factor until active slope failure is detected. The factor directly applies to the maximum allowable value of shear stress τ_{max} (see Eq. (2.9)). The reduction factor at the verge of slope collapse is defined as the FOS based on the proposed (local strength reduction) technique.

Although, in theory, it is possible to find a best fit to match the reduced envelope with a Hoek-Brown type equation (see, e.g., Hammah et al. 2005), this step is not required with this particular model implementation because the logic relies on the direct use of envelope tangent (there is no need to define a curve and then the tangent when the tangent is available in the first place – see above). Also, the proposed local strength reduction technique provides a means by which to quantify the shear stress allowance to collapse, as one would expect. In this case, the reduction factor is not applied directly to model parameters.

FOS with respect to Unconfined Compressive Strength, σ_{ci}

A factor-of-safety calculation based on an intact unconfined compressive strength, σ_{ci}, reduction technique is also available. The intact unconfined compressive strength is reduced by a reduction factor until active failure is detected. This particular measure is introduced to allow comparison with stability charts for simple slopes obtained by Li et al. (2008), using numerical limit analysis (see Section 2.5.2.2).

2.4.1.4 Coulomb Joints

Joint strengths can be included in the safety-factor calculation by assigning Coulomb joint material with **block contact cmodel assign area**. By default, joint cohesion and friction angle are included when **block factor-of-safety** is issued. The strength reduction equations for these properties are

$$c_i^{trial} = \frac{1}{F^{trial}} c_i \tag{2.16}$$

$$\phi_i^{trial} = \arctan\left(\frac{1}{F^{trial}} \tan \phi_i \right) \tag{2.17}$$

Joint tensile strength can be included by adding **interface include tension**, and joint strength properties can be included or excluded with the keywords **interface include/exclude cohesion**, **friction** and **tension**.

2.4.2 Structural Elements

The strength reduction technique can be selected for structural elements. When **structure include** keywords are given, several strength properties are affected:

grout shear strength and axial compressive and tensile strength of cable elements;

axial and shear ultimate load limits of local reinforcement;

axial compressive and tensile yield strengths of liner surface elements; and

axial compressive load limit for support elements.

These strength properties are reduced in the same manner as the other strength properties when **block factor-of-safety include structure** is issued. For example, for cable grout strength values c_g and ϕ_g, the strength-reduction equations are

$$c_g^{trial} = \frac{1}{F^{trial}} c_g \tag{2.18}$$

$$\phi_g^{trial} = \arctan\left(\frac{1}{F^{trial}} \tan \phi_g \right) \tag{2.19}$$

2.5 Example FOS Calculations Using the Strength Reduction Method

2.5.1 Failure Modes of a Simple Slope in Jointed Mohr-Coulomb Material

Factor-of-safety calculations using the strength reduction method in *UDEC* can determine both the safety factor and the mode of failure of a slope in a jointed rock mass. Several models are run in this section to illustrate the different types of failure modes that can be identified from a factor-of-safety calculation. Modes of failure include rock mass failure in a homogeneous and unjointed rock slope, plane failure of slopes containing either daylighting or non-daylighting discontinuities, and block and flexural toppling failure involving either forward or backward toppling of blocks.*

The jointed rock failure modes presented in this section assume the joint structure can be represented as a system of discrete blocks. Failure modes involving joints that terminate within intact rock, such as step-path failure, can also be simulated with *UDEC*. For an example, see Section 13 in the **Example Applications**.

A simple slope geometry is used for all of the stability analysis cases described in this section. The slope has a height of 260 m and slope angle of 55°. The rock blocks in the model are represented as deformable Mohr-Coulomb material, and the discontinuities behave as Coulomb joint material. A maximum zone size of 15 m is assigned for the deformable blocks in all models. The model slope geometry used for all cases is shown in Figure 2.1.

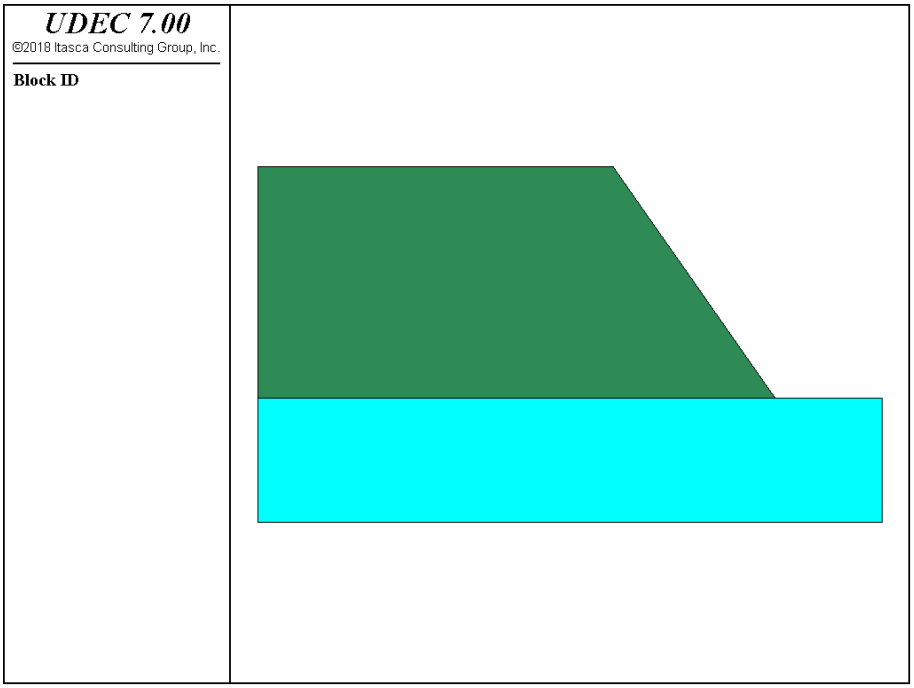

Figure 2.1 Slope geometry

* These slope models and modes of failure are also described in detail by Lorig and Varona (2004).

Six slope stability cases are analyzed. The cases include one model with no joint structure, three models with one joint set, and two models with two joint sets. The rock block properties and joint properties for the six cases are listed in Table 2.1.

Table 2.1 Slope stability cases

Soil Property	Case 1	Case 2	Case 3	Case 4	Case 5	Case 6
Rock Density (kg/m^3)	2660	2660	2660	2660	2660	2660
Rock Bulk Modulus (GPa)	6.3	6.3	6.3	6.3	6.3	6.3
Rock Shear Modulus (GPa)	3.6	3.6	3.6	3.6	3.6	3.6
Rock Cohesion (kPa)	675	675	675	675	675	10^{10}
Rock Tension (kPa)	0	0	0	0	0	10^{10}
Rock Friction (degrees)	43	43	43	43	43	43
Joint Set 1 Dip (degrees)	–	145	110	70	70	125
Joint Set 1 Spacing (m)	–	10	20	20	20	10
Joint Set 1 Friction (degrees)	–	40	40	40	40	40
Joint Set 1 Cohesion (kPa)	–	100	0	0	0	0
Joint Set 1 Stiffness (GPa/m)	–	1	1	1	1	1
Joint Set 2 Dip (degrees)	–	–	–	–	340	0
Joint Set 2 Spacing (m)	–	–	–	–	30	40
Joint Set 2 Friction (degrees)	–	–	–	–	40	40
Joint Set 2 Cohesion (kPa)	–	–	–	–	0	0
Joint Set 2 Stiffness (GPa/m)	–	–	–	–	1	1

The cases illustrate six different failure conditions. They are discussed separately in the following pages. The command listing for the six cases is given in Example 2.1.

Case 1: unjointed, homogeneous rock – rock mass failure

For Case 1 the slope is a homogeneous rock without joints. Failure of the slope primarily involves shearing though the rock mass, and the shear failure surface is approximately circular as shown in Figure 2.2. For the Case 1 rock properties listed in Table 2.1, a factor of safety of 1.65 is calculated. Note that the failure surface in a *UDEC* model can usually be most clearly identified from a plot of velocity vectors, and either a displacement or velocity contour plot. In Figure 2.2, velocity vectors and x-velocity contours clearly show the failure surface.

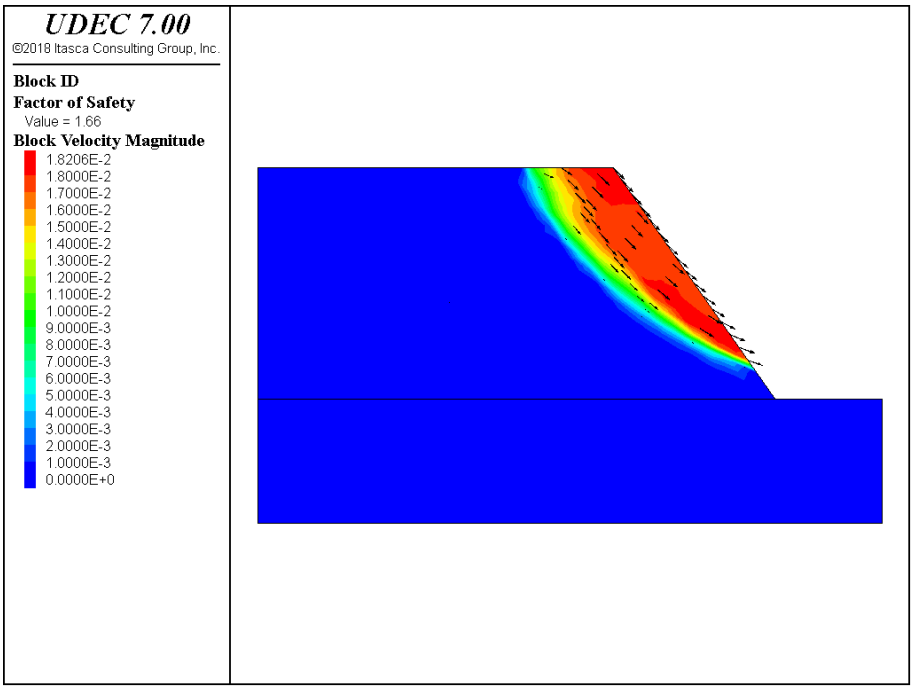

Figure 2.2 Case 1 – rock mass failure

Case 2: daylighting joint structure – plane failure

In the Case 2 simulation, a single joint set is added to the model. The joints dip at 145° (i.e., daylighting out of the slope at 35°) and are spaced at 20 m. The failure mechanism that develops combines sliding along joints near the slope toe with tensile failure of the blocks near the top of the slope. Figure 2.3 shows the failure surface. The calculated factor of safety is 1.30 for this case.

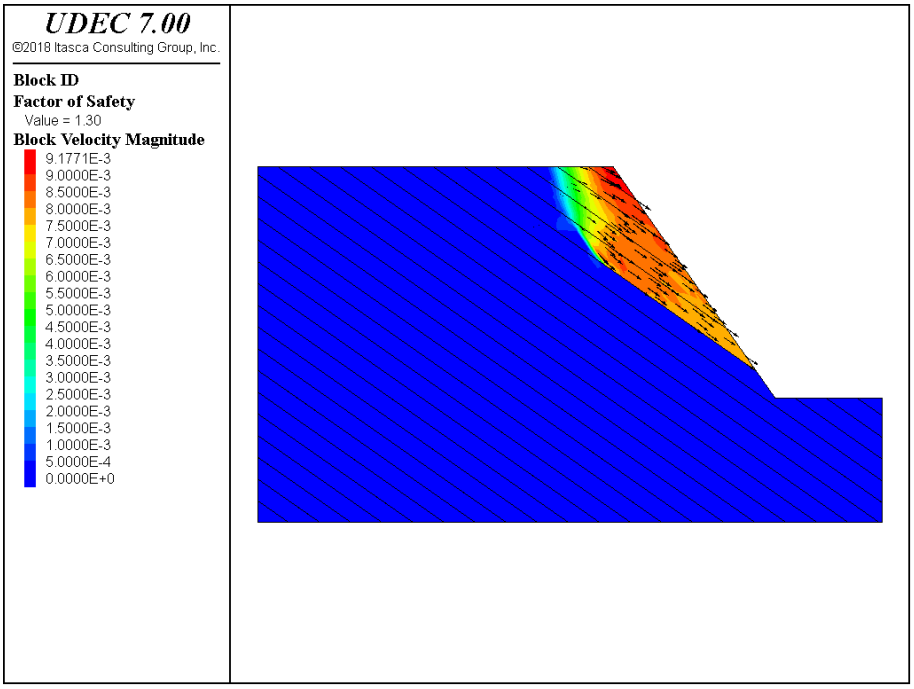

Figure 2.3 Case 2 – plane failure in slope with daylighting joints

Case 3: non-daylighting joint structure – plane failure

In the third case, the dip angle of the single joint set is set to 110° (or 70° in the same direction as the slope). This produces non-daylighting joints along the slope face. The joint spacing is 20 m. The failure mode that develops in this case involves sliding along the discontinuities, and shearing through the rock blocks at the toe of the slope. Figure 2.4 illustrates the failure mechanism. The resulting factor of safety is 1.56 for the given problem conditions.

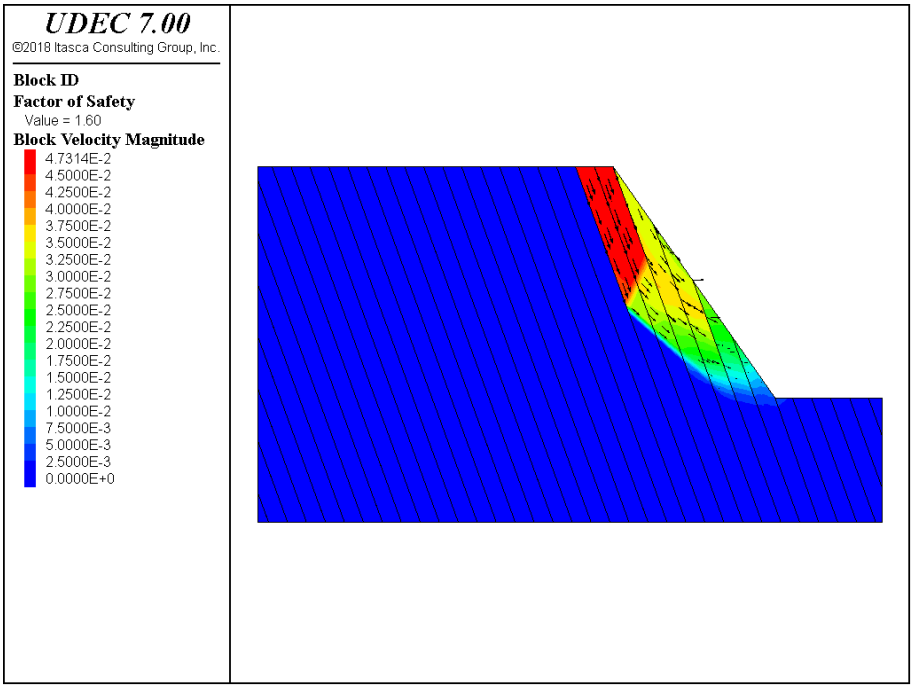

Figure 2.4 Case 3 – plane failure in slope with non-daylighting joints

Case 4: joints dipping into the slope – flexural toppling failure

The joint set is oriented at a dip angle of 70° and spaced at 20 m in Case 4. This results in joints dipping steeply into the slope face. The joints form columns that tend to bend out of the slope, and result in a flexural toppling failure mode. Figure 2.5 shows the failure surface, and Figure 2.6 illustrates the flexural toppling mode from a magnified view of the block deformation. The calculated factor of safety is 1.36.

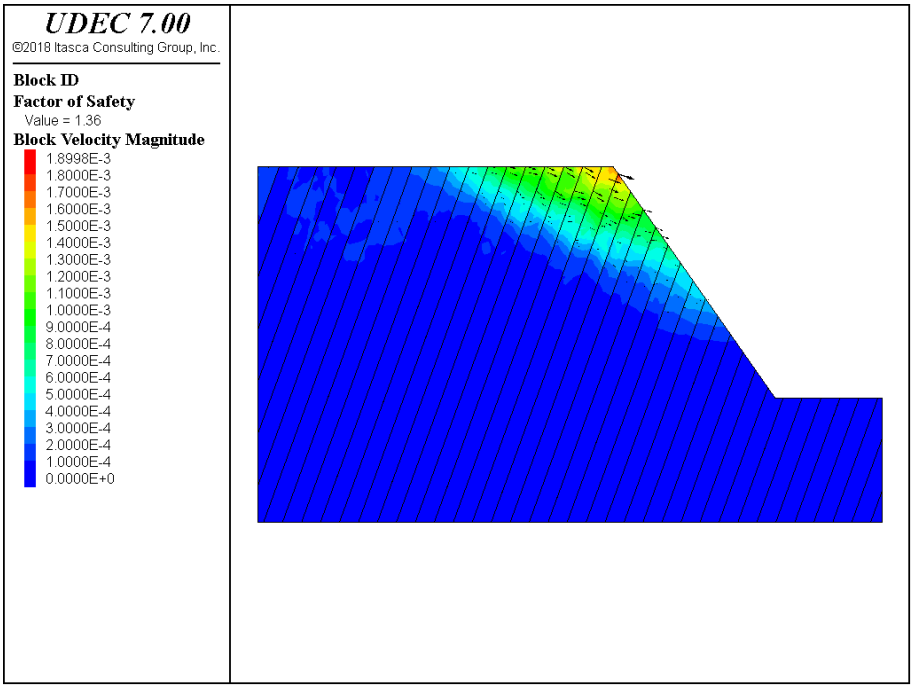

Figure 2.5 Case 4 – flexural toppling failure for joints dipping into the slope

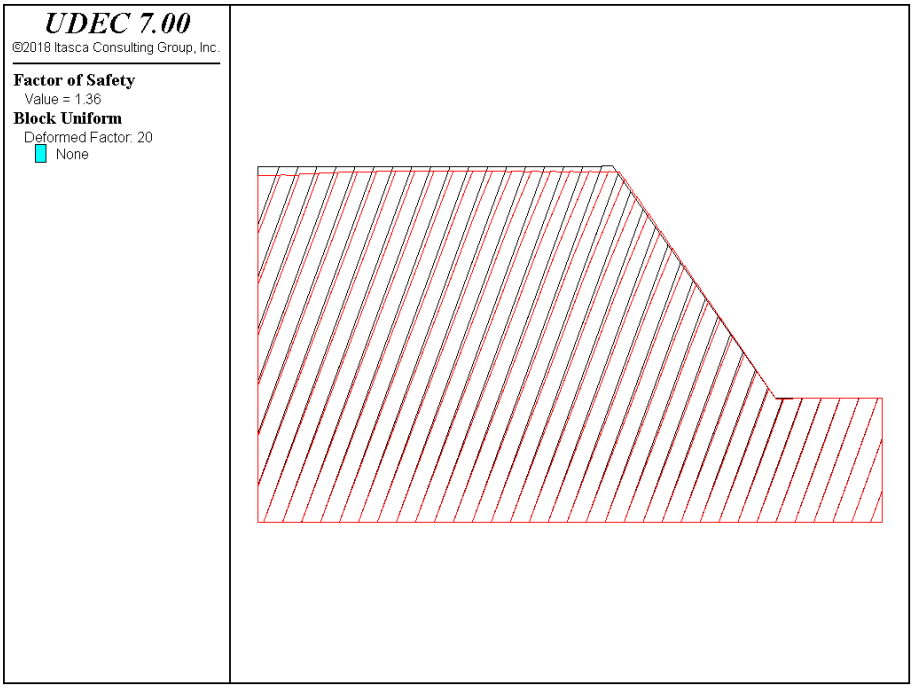

Figure 2.6 Case 4 – flexural toppling mode identified from magnified block deformation

Case 5: two orthogonal joint sets – forward block toppling failure

The slope contains two orthogonal joint sets in Case 5. One set dips at 70° with a spacing of 20 m, and a cross-joint set dips at −20° with a spacing of 30 m. The cross-joints provide release surfaces for rotation of the blocks. The blocks, driven by self-weight, rotate forward out of the slope. Figure 2.7 shows the failure surface for the Case 5 conditions. The calculated factor of safety is 1.11. The magnified block deformation plot in Figure 2.8 illustrates the forward block rotation out of the slope.

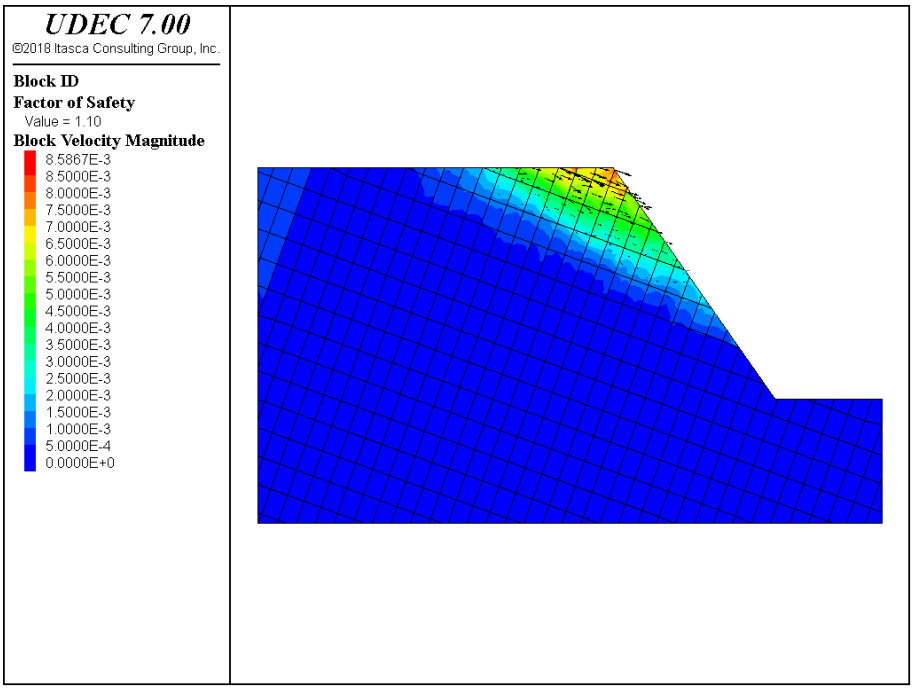

Figure 2.7 Case 5 – forward block toppling failure for a slope with two joint sets

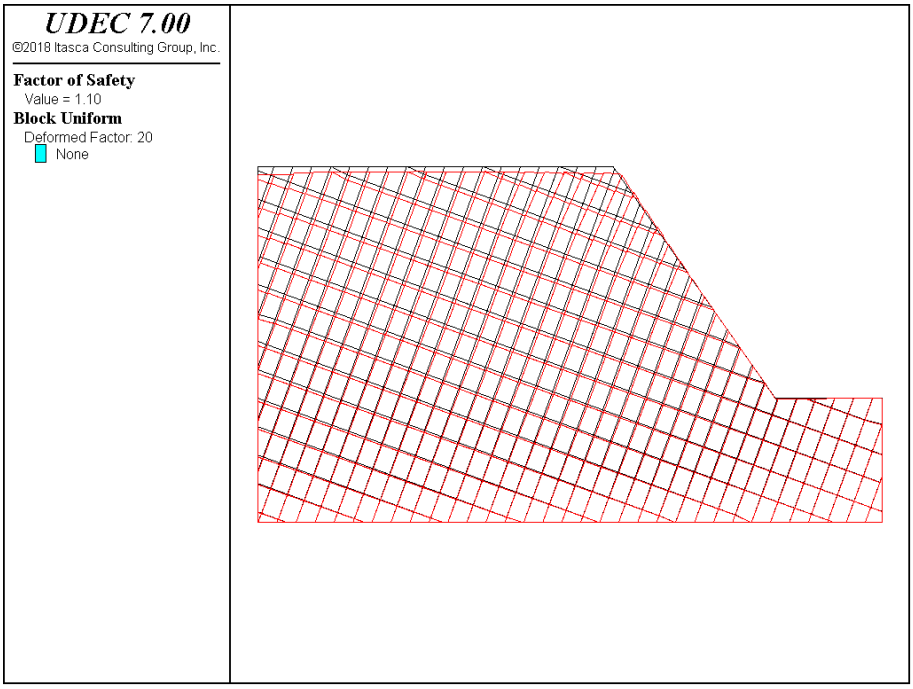

Figure 2.8 Case 5 – forward block toppling mode identified from magnified block deformation

Case 6: two orthogonal joint sets – reverse (backward) block toppling failure

Backward or reverse block toppling failure of a slope can occur when joints parallel to the slope face and flatter cross-joints are particularly weak. In Case 6, one joint set is oriented at 125° (i.e., parallel to the slope face) with a spacing of 10 m. A cross-joint set is horizontal and spaced at 40 m. Note that in this case, in order to highlight the failure mode, elastic material behavior is prescribed for the rock blocks. Figure 2.9 displays the reverse toppling failure mode. The calculated factor of safety is 1.75. The backward block toppling mode is clearly seen in the magnified block deformation plot in Figure 2.10.

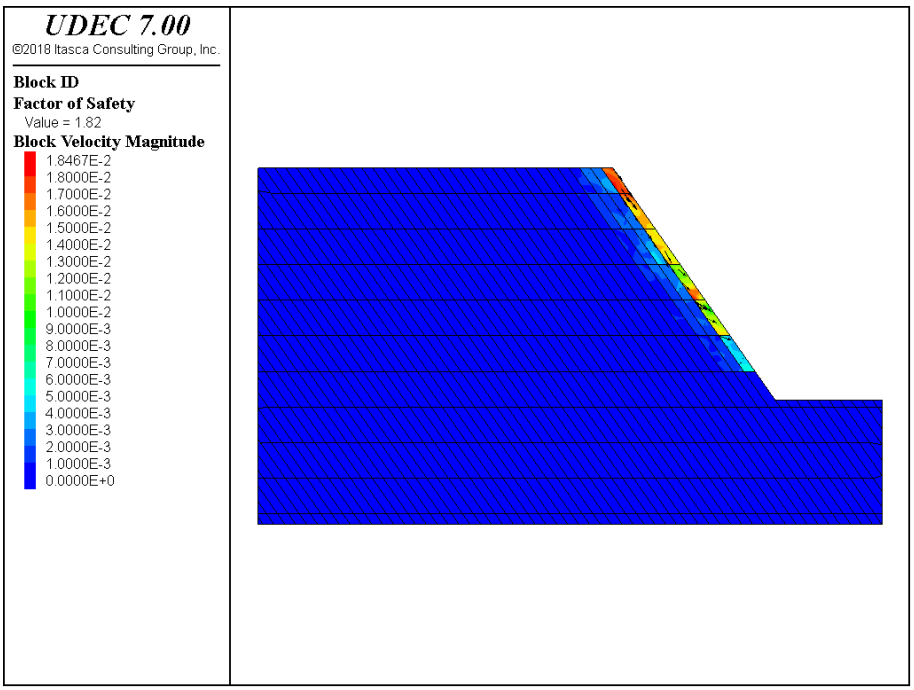

Figure 2.9 Case 6 – reverse block toppling failure for a slope with two joint sets

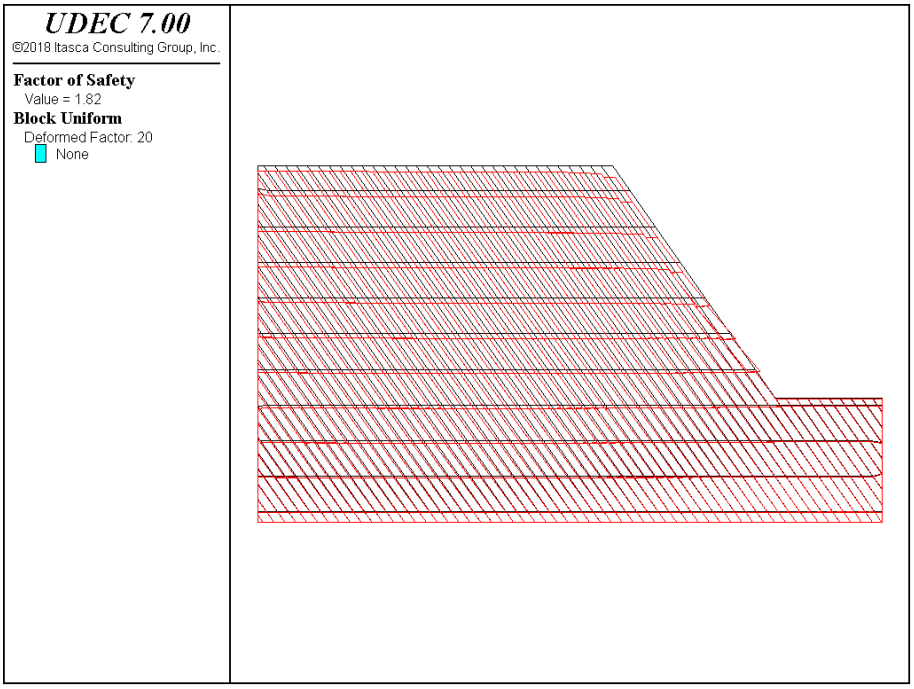

Figure 2.10 Case 6 – reverse block toppling mode identified from magnified block deformation

Example 2.1 Failure modes of a simple slope in jointed Mohr-Coulomb material

```
model new
; Failure Modes of a Simple Slope
; Case 1
block tolerance corner-round-length 0.7
block tolerance minimum-edge-length 1.4
block create polygon 0,0 0,400 398,400 580,140 700,140 700,0
block cut crack (0,140) (580,140) join
block zone gen quad 15.0
block zone group 'rock'
block zone cmodel assign mohr-c density 2.66E3 bulk 6.3E9 ...
  shear 3.6E9 friction 43 ...
  cohesion 6.75E5 range group 'rock'
block contact group 'joint'
block contact cmodel assign area stiffness-shear 1E9 ...
  stiffness-normal 1E9 friction 40 cohesion 1E5 range group 'joint'
; new contact default
block contact cmodel default area stiffness-shear=1E9 ...
  stiffness-normal=1E9 friction=40 cohesion=1E5
bl grid app velocity-x 0 range pos-x -0.1,0.1    pos-y -0.1,400.1
bl grid app velocity-x 0 range pos-x 699.9,700.1 pos-y -0.1,140.1
bl grid app velocity-x 0 range pos-x -0.1,700.1  pos-y -0.1,0.1
bl grid app velocity-y 0 range pos-x -0.1,700.1  pos-y -0.1,0.1
block mechanical gravity=0.0 -9.81
block solve elastic
model save 't1.sav'

block largestrain off
block mech reset  vel disp
block factor-of-safety no_restore file='FoSmode1.fsv'
;
; Case 2
model new
block tolerance corner-round-length 0.7
block tolerance minimum-edge-length 1.4
block create polygon 0,0 0,400 398,400 580,140 700,140 700,0
block cut joint-set angle 145 spacing 20 origin 0,0
block zone gen quad 15.0
block zone gen edge 15.0
block zone group 'rock'
block zone cmodel assign mohr-c density 2.66E3 bulk 6.3E9 ...
  shear 3.6E9 friction 43 cohesion 6.75E5 range group 'rock'
block contact group 'joint'
block contact cmodel assign area stiffness-shear 1E9 ...
```

```
  stiffness-normal 1E9 friction 40 cohesion 1E5 range group 'joint'
; new contact default
block contact cmodel default area stiffness-shear=1E9 ...
  stiffness-normal=1E9 friction=40 cohesion=1E5
bl grid app velocity-x 0 range pos-x -0.1,0.1    pos-y -0.1,400.1
bl grid app velocity-x 0 range pos-x 699.9,700.1 pos-y -0.1,140.1
bl grid app velocity-x 0 range pos-x -0.1,700.1  pos-y -0.1,0.1
bl grid app velocity-y 0 range pos-x -0.1,700.1  pos-y -0.1,0.1
block mechanical gravity=0.0 -9.81
block solve elastic
model save 't2.sav'

block mech reset vel disp
block largestrain off
block factor-of-safety no_restore file='FoSmode2.fsv'
;
; Case 3
model new
block tolerance corner-round-length 0.7
block tolerance minimum-edge-length 1.4
block create polygon 0,0 0,400 398,400 580,140 700,140 700,0
block cut joint-set angle 110 spacing 20 origin 12,0
block zone gen quad 15.0
block zone gen edge 15.0
block zone group 'rock'
block zone cmodel assign mohr-c density 2.66E3 bulk 6.3E9 ...
  shear 3.6E9 friction 43 ...
 cohesion 6.75E5 range group 'rock'
block contact group 'joint'
block contact cmodel assign area stiffness-shear 1E9 ...
  stiffness-normal 1E9 friction 40 cohesion 0 range group 'joint'
; new contact default
block contact cmodel default area stiffness-shear=1E9 ...
  stiffness-normal=1E9 friction=40 cohesion=0
bl grid app velocity-x 0 range pos-x -0.1,0.1    pos-y -0.1,400.1
bl grid app velocity-x 0 range pos-x 699.9,700.1 pos-y -0.1,140.1
bl grid app velocity-x 0 range pos-x -0.1,700.1  pos-y -0.1,0.1
bl grid app velocity-y 0 range pos-x -0.1,700.1  pos-y -0.1,0.1
block mechanical gravity=0.0 -9.81
block solve elastic
model save 't3.sav'

block mech reset  vel disp
block largestrain off
block factor-of-safety no_restore file='FoSmode3.fsv'
;
```

```
; Case 4
model new
block tolerance corner-round-length 0.7
block tolerance minimum-edge-length 1.4
block create polygon 0,0 0,400 398,400 580,140 700,140 700,0
block cut joint-set angle 70 spacing 20 origin 6,0
block zone gen quad 15.0
block zone gen edge 15.0
block zone group 'rock'
block zone cmodel assign mohr-c density 2.66E3 bulk 6.3E9 ...
  shear 3.6E9 friction 43 cohesion 6.75E5 range group 'rock'
block contact group 'joint'
block contact cmodel assign area stiffness-shear 1E9 ...
  stiffness-normal 1E9 friction 40 cohesion 0 range group 'joint'
; new contact default
block contact cmodel default area stiffness-shear=1E9 ...
  stiffness-normal=1E9 friction=40 cohesion=0
bl grid app velocity-x 0 range pos-x -0.1,0.1    pos-y -0.1,400.1
bl grid app velocity-x 0 range pos-x 699.9,700.1 pos-y -0.1,140.1
bl grid app velocity-x 0 range pos-x -0.1,700.1  pos-y -0.1,0.1
bl grid app velocity-y 0 range pos-x -0.1,700.1  pos-y -0.1,0.1
block mechanical gravity=0.0 -9.81
block solve elastic
model save 't4.sav'

block factor-of-safety no_restore file='FoSmode4.fsv'
;
; Case 5
model new
block tolerance corner-round-length 0.7
block tolerance minimum-edge-length 1.4
block create polygon 0,0 0,400 398,400 580,140 700,140 700,0
block cut joint-set angle 70 spacing 20 origin 0,0
block cut joint-set angle 340 spacing 30 origin 0,12
block zone gen quad 15.0
block zone gen edge 15.0
block zone group 'rock'
block zone cmodel assign mohr-c density 2.66E3 bulk 6.3E9 ...
  shear 3.6E9 friction 43 cohesion 6.75E5 range group 'rock'
block contact group 'joint'
block contact cmodel assign area stiffness-shear 1E9 ...
  stiffness-normal 1E9 friction 40 cohesion 0 range group 'joint'
; new contact default
block contact cmodel default area stiffness-shear=1E9 ...
  stiffness-normal=1E9 friction=40 cohesion=0
bl grid app velocity-x 0 range pos-x -0.1,0.1    pos-y -0.1,400.1
```

```
bl grid app velocity-x 0 range pos-x 699.9,700.1 pos-y -0.1,140.1
bl grid app velocity-x 0 range pos-x -0.1,700.1  pos-y -0.1,0.1
bl grid app velocity-y 0 range pos-x -0.1,700.1  pos-y -0.1,0.1
block mechanical gravity=0.0 -9.81
block solve elastic
model save 't5.sav'

block mech reset  vel disp
block largestrain off
block factor-of-safety no_restore file='FoSmode5.fsv'
;
; Case 6
model new
block tolerance corner-round-length 0.7
block tolerance minimum-edge-length 1.4
block create polygon 0,0 0,400 398,400 580,140 700,140 700,0
block cut joint-set angle 125 spacing 10 origin 6,0
block cut joint-set angle 0 spacing 40 origin 0,12
block zone gen quad 15.0
block zone gen edge 15.0
block zone group 'rock'
block zone cmodel assign mohr-c density 2.66E3 bulk 6.3E9 ...
  shear 3.6E9 friction 43 cohesion 6.75E10 tension 6.75e10 ...
  range group 'rock'
block contact group 'joint'
block contact cmodel assign area stiffness-shear 1E9 ...
  stiffness-normal 1E9 friction 40 cohesion 0 range group 'joint'
; new contact default
block contact cmodel default area stiffness-shear=1E9 ...
  stiffness-normal=1E9 friction=40 cohesion=0
bl grid app velocity-x 0 range pos-x -0.1,0.1    pos-y -0.1,400.1
bl grid app velocity-x 0 range pos-x 699.9,700.1 pos-y -0.1,140.1
bl grid app velocity-x 0 range pos-x -0.1,700.1  pos-y -0.1,0.1
bl grid app velocity-y 0 range pos-x -0.1,700.1  pos-y -0.1,0.1
block mechanical gravity=0.0 -9.81
block largestrain off
block solve elastic
model save 't6.sav'

block mech reset vel disp
block factor-of-safety no_restore file='FoSmode6.fsv'
```

2.5.2 Verification Tests for a Simple Slope in Hoek-Brown Material

Two verification exercises are performed to validate the factor-of-safety calculation using Hoek-Brown material in *UDEC*. The first exercise tests the strength-reduction calculation based upon shear strength, τ; the second exercise tests the calculation based upon intact, unconfined compressive strength (see Section 2.4.1.3).

2.5.2.1 Factor of Safety with respect to Shear Strength

The factor of safety with respect to Hoek-Brown shear strength is calculated for a simple slope geometry, and compared to results based upon other methods to calculate a safety factor for Hoek-Brown material (i.e., generalized Hoek-Brown, equivalent Mohr-Coulomb, and Bishop and Spencer limit equilibrium methods) reported by Hammah et al. (2005). The rock slope for this comparison calculation has an inclination of 45° and a height of 10 m. The rock is represented as a Hoek-Brown material with the following properties:

$$
\begin{aligned}
E &= 5000 \text{ MPa} \\
\nu &= 0.3 \\
\rho &= 2500 \text{ kg/m}^3 \\
m_b &= 0.067 \\
s &= 0.000025 \\
a &= 0.619 \\
\sigma_{ci} &= 30 \text{ MPa}
\end{aligned}
$$

The *UDEC* model mesh used for this test is shown in Figure 2.11. The model contains a horizontal construction joint at the toe of the slope to allow use of **block zone generate quad** zoning. The maximum zone width is set to 1 m.*

By default, when **block factor-of-safety** is executed for a *UDEC* model with **block zone cmodel assign hoek-brown**, the factor of safety calculation is performed for Hoek-Brown material with respect to shear strength. The calculated factor of safety for this test is 1.16. The failure surface is shown by the displacement magnitude contour plot in Figure 2.12. The result compares well with the results reported by Hammah et al. (2005). Table 2.2 summarizes the safety factors reported for this test.

---

* Note that **block zone generate edge** triangular zones will also produce the same solution accuracy for this example, provided that the **block zone nodal-mixed-discretization on** command is given to implement nodal mixed discretization.

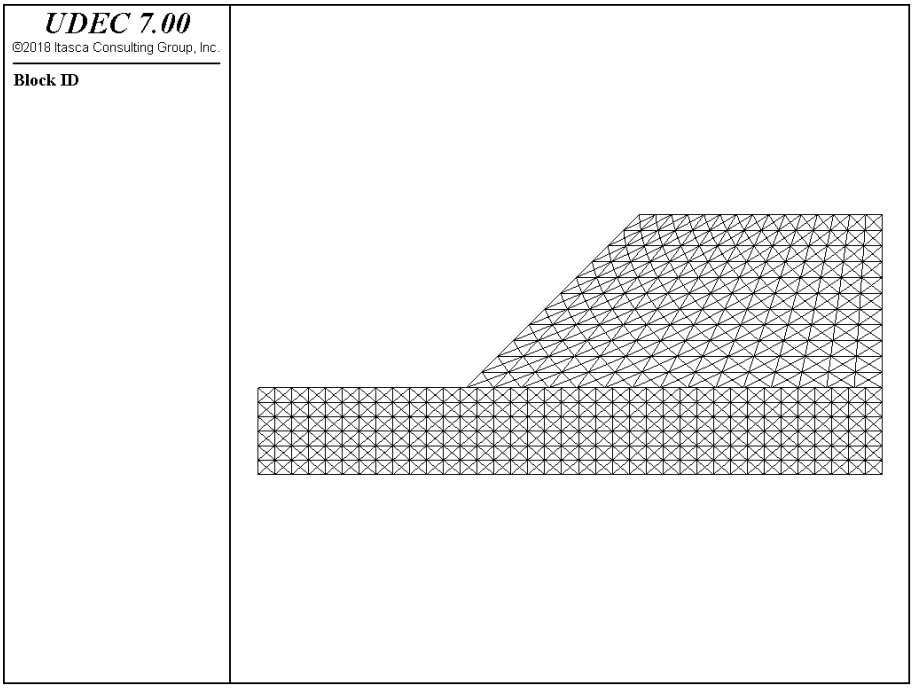

Figure 2.11 Slope model mesh

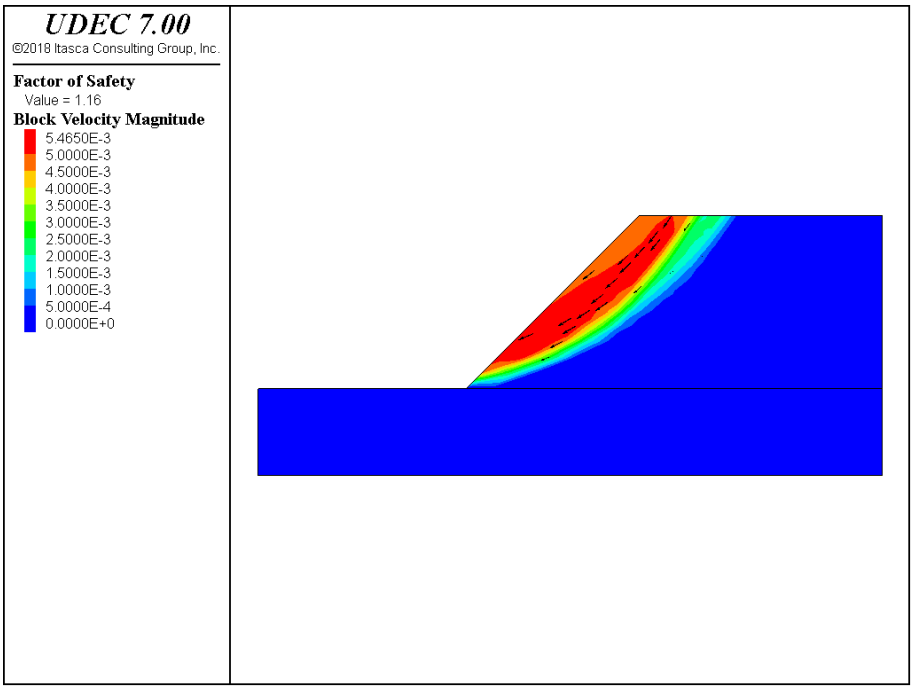

Figure 2.12 Factor of safety and failure surface calculated for simple slope in Hoek-Brown material

Table 2.2 Factor-of-safety results for Hoek-Brown slope

Method	Factor of Safety
Hoek-Brown model with respect to shear strength	1.15
generalized Hoek-Brown strength reduction*	1.15
equivalent Mohr-Coulomb strength reduction*	1.15
Bishop's simplified limit equilibrium*	1.153
Spencer's limit equilibrium*	1.152

* from Hammah et al. (2005)

Hammah et al. (2005) also report the results for the case in which a horizontal layer of Mohr-Coulomb material is located at the toe of the slope. The layer is 1 m thick, and has zero cohesion and 25° friction. The slope with the Mohr-Coulomb layer is shown in Figure 2.13.

When **block factor-of-safety** is issued, the strength reduction method is performed concurrently for Hoek-Brown material (as described in Section 2.4.1.3) and Mohr-Coulomb material (as described in Section 2.4.1.1). The factor of safety calculated for this model is 1.0. The results are shown in Figure 2.14.

Table 2.3 compares the *UDEC* result with results from other methods reported by Hammah et al. (2005). The *UDEC* result is approximately 4% higher.

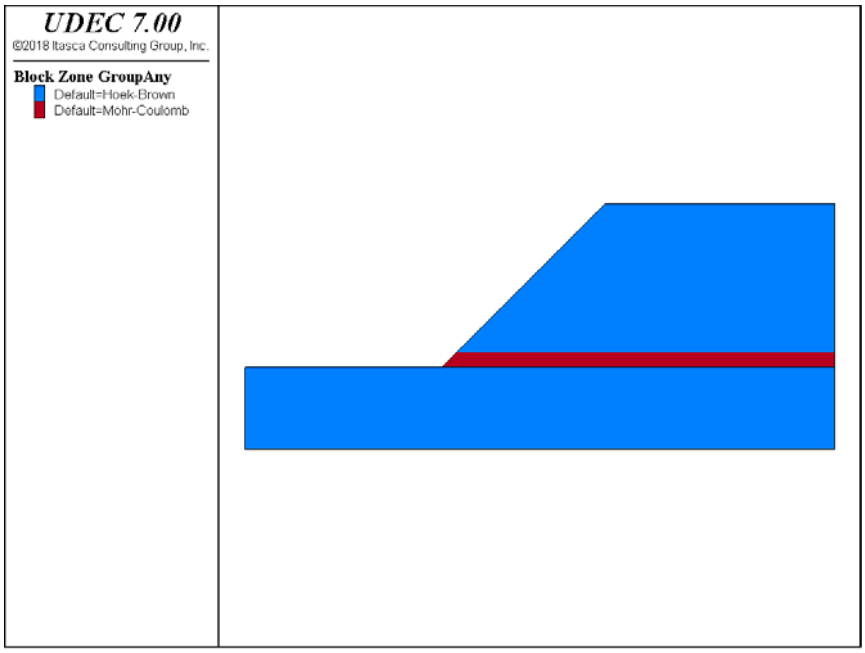

Figure 2.13 Simple slope in Hoek-Brown material with a Mohr-Coulomb layer

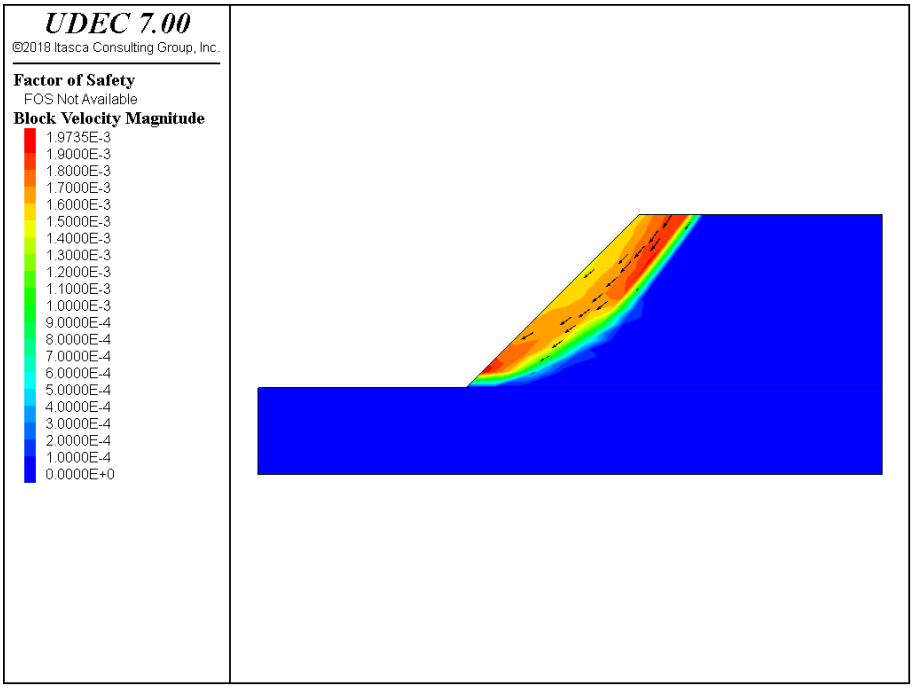

Figure 2.14 Factor of safety and failure surface calculated for simple slope in Hoek-Brown material with Mohr-Coulomb layer

Table 2.3 Hoek-Brown slope with Mohr-Coulomb layer

Method	Factor of Safety
Hoek-Brown model wrt shear strength & Mohr-Coulomb model	1.00
generalized Hoek-Brown strength reduction*	0.96
Bishop's simplified limit equilibrium*	0.934
Spencer's limit equilibrium*	0.963

* from Hammah et al. (2005)

Example 2.2 lists the *UDEC* commands for these two problems.

Example 2.2 Factor of safety with respect to shear strength for Hoek-Brown material

```
model new
;file: hb1slope.dat
; Hoek-Brown material
block tolerance corner-round-length 3.6E-2
block tolerance minimum-edge-length 7.2E-2
block create polygon 0,0 0,5 12,5 22,15 36,15 36,0
block cut crack (12,5) (36,5) join
```

```
block zone gen quad 1.0
block zone group 'Hoek-Brown'
block zone cmodel assign hoek-brown density 2.5E-3 bulk 4.167E3 ...
  shear 1.923E3 constant-mb 6.7E-2 constant-s 2.5E-5 ...
  constant-a 0.619 constant-sci 30 flag-fos 0 tension = 3.0 ...
  range group 'Hoek-Brown'
bl grid app velocity-x 0 range pos-x -0.1,0.1  pos-y -0.1,5.1
bl grid app velocity-x 0 range pos-x 35.9,36.1 pos-y -0.1,15.1
bl grid app velocity-x 0 range pos-x -0.1,36.1 pos-y -0.1,0.1
bl grid app velocity-y 0 range pos-x -0.1,36.1 pos-y -0.1,0.1
block mechanical gravity=0.0 -10.0
model save 'hb1a.sav'
block factor-of-safety no_restore file='FoSmodehb1a.fsv'
;
; Hoek-Brown material with Mohr-Coulomb layer
model new
block tolerance corner-round-length 3.6E-2
block tolerance minimum-edge-length 7.2E-2
block create polygon 0,0 0,5 12,5 22,15 36,15 36,0
; block cut crack (12,6) (36,6) join
block cut crack (12,5) (36,5) join
block zone gen quad 1.0
block zone group 'Hoek-Brown'
block zone cmodel assign hoek-brown density 2.5E-3 bulk 4.167E3 ...
  shear 1.923E3 constant-mb 6.7E-2 constant-s 2.5E-5 ...
  constant-a 0.619 constant-sci 30 flag-fos 0 tension = 3.0 ...
  range group 'Hoek-Brown'
block zone group 'Mohr-Coulomb' range pos-x 12,36 pos-y 5,6
block zone cmodel assign mohr-c density 2.5E-3 bulk 4.167E3 ...
  shear 1.923E3 friction 25 range group 'Mohr-Coulomb'
bl grid app velocity-x 0 range pos-x -0.1,0.1  pos-y -0.1,5.1
bl grid app velocity-x 0 range pos-x 35.9,36.1 pos-y -0.1,15.1
bl grid app velocity-x 0 range pos-x -0.1,36.1 pos-y -0.1,0.1
bl grid app velocity-y 0 range pos-x -0.1,36.1 pos-y -0.1,0.1
block mechanical gravity=0.0 -10.0
model save 'hb1b.sav'

block factor-of-safety no_restore file='FoSmodehb1b.fsv'
```

2.5.2.2 Stability Numbers for a Simple Slope

Consider the case of a simple slope in a Hoek-Brown material with height, H, slope angle, β, and unit weight, γ. It can be shown, using dimensional analysis, that the shear strength reduction technique for computing F_s will produce a relation of the form

$$F_s = f_1(N, \beta, m_b, s, a) \tag{2.20}$$

where the stability number (similarity parameter) N is defined as

$$N = \frac{\sigma_{ci}}{\gamma H} \tag{2.21}$$

In other words, F_s is not necessarily proportional to N.

Limit analysis (upper-bound solution) provides the functional relation (see Chen 2007 and Dawson et al. 2000)

$$\frac{\gamma H_{cr}}{\sigma_{ci}} = f_2(\beta, m_b, s, a) \tag{2.22}$$

where H_{cr} is the slope critical height (height to bring the slope to the verge of failure). If the factor of safety is defined with respect to height, $F_H = H_{cr}/H$, and Eq. (2.22) gives

$$F_H = N f_2(\beta, m_b, s, a) \tag{2.23}$$

In this case, the factor of safety, F_H, is proportional to the similarity parameter, N. Also, the same proportionality property applies if the factor of safety is defined with respect to unit weight, $F_\gamma = \gamma_{cr}/\gamma$, or for that matter, with respect to intact unconfined compressive strength, $F_{\sigma_{ci}} = \sigma_{ci}/\sigma_{ci|cr}$.

Some notes follow from this observation:

1. The FOS value for a simple slope derived from limit analysis (upper-bound solution) can be considered as taken with respect to intact unconfined compressive strength. Also, this particular FOS value can be estimated by applying the strength reduction technique on σ_{ci}.

2. FOS with respect to shear strength and FOS traditionally associated with stability numbers in charts correspond to different measures of safety, and do not generally coincide away from 1. In fact, in the literature, FOS results obtained using limit analysis and limit equilibrium analysis are, typically, only compared in close vicinity of 1, where both measures coincide.

3. FOS with respect to shear strength for Hoek-Brown material is not related linearly to stability number, even in the case of a simple slope.

For these reasons then, an absolute statement such as "a factor of safety above 1.2 is considered acceptable for the slope" should be considered meaningless, unless the FOS measure is precisely defined, and its value is used in a comparison analysis.

The application example for a simple slope, reported by Li et al. (2008), is used to compare the strength reduction calculation with respect to intact unconfined compressive strength to the limit analysis solution. The slope has a height of 25 m and slope angle of 60°. The rock has the following properties:

intact unconfined compressive strength, σ_{ci}	=	20 MPa
Geological Strength Index, GSI	=	30
intact material constant, m_i	=	8.0
degree of disturbance, D	=	0
unit weight, γ	=	23 kN/m^3

Hoek-Brown properties are determined from the GSI, m_i and D properties through the following equations:

$$m_b = m_i \exp\left(\frac{GSI - 100}{28 - 14D}\right) \tag{2.24}$$

$$s = \exp\left(\frac{GSI - 100}{9 - 3D}\right) \tag{2.25}$$

$$a = \frac{1}{2} + \frac{1}{6}\left(e^{-GSI/15} - e^{-20/3}\right) \tag{2.26}$$

The value for the stability number, N, is (from Eq. (2.21)) equal to 34.8. Li et al. (2008) provide charts for a slope stability number, N/F, as a function of, m_i and GSI. For the application example, N/F = 4.3. The factor of safety, F, is then equal to F = 34.8/4.3 = 8.1.

This example is run with *UDEC* using **block zone cmodel assign hoek-brown**, and setting **block zone property flag-fos** = 1 in order to have the strength reduction calculation with respect to σ_{ci}. The data file for this example is listed in Example 2.3. The failure surface calculated by *UDEC* is shown in Figure 2.15. The calculated factor of safety is 7.7, which differs from the limit analysis solution by approximately 5%.

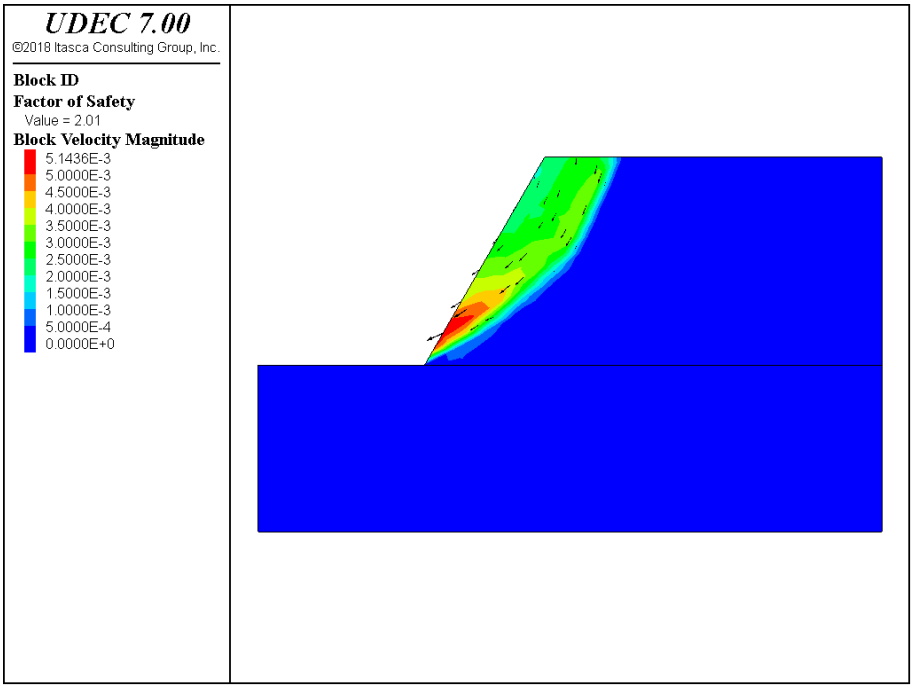

Figure 2.15 Factor of safety and failure surface calculated for simple slope in Hoek-Brown material (strength reduction with respect to intact unconfined compressive strength)

Example 2.3 Factor of safety with respect to intact unconfined compressive strength for Hoek-Brown material

```
model new
;file: hb2slope.dat
; Factor of Safety with respect to UCS
block tolerance corner-round-length 7.5E-2
block tolerance minimum-edge-length 0.15
block create polygon 0,0 0,20 20,20 34.43,45 75,45 75,0
block cut crack (20,20) (75,20) join
block zone gen quad 2.0
block zone group 'Hoek-Brown'
block zone cmodel assign mhoekbrown density 2.3E3 bulk 4.1667E9 ...
  shear 1.923E9 constant-mb 0.6567 constant-s 4.189E-4 ...
  constant-a 0.5223 constant-sci 2E7 tension = 2e6 ...
  range group 'Hoek-Brown'
bl grid app velocity-x 0 range pos-x -0.1,0.1  pos-y -0.1,20.1
bl grid app velocity-x 0 range pos-x 74.9,75.1 pos-y -0.1,45.1
bl grid app velocity-x 0 range pos-x -0.1,75.1 pos-y -0.1,0.1
bl grid app velocity-y 0 range pos-x -0.1,75.1 pos-y -0.1,0.1
block mechanical gravity=0.0 -10.0
block largestrain off
model save 'hb2.sav'
;
block zone prop flag-fos 1
block factor-of-safety no_restore file 'FoSmodehb2.fsv'
```

2.5.3 Factor-of-Safety Contours

Typically, application of the strength reduction method produces one single factor of safety per simulation, corresponding to one global minimum stability state. However, the ability to calculate multiple minimum states may be of interest, for example, along a complex slope profile such as a benched cut or a slope with a berm (e.g., see Cheng et al. 2007). A "safety map" may be constructed through a series of analyses using the limit equilibrium method to identify multiple possible failure surfaces for slopes of this type (Baker and Leshchinsky 2001).

The explicit dynamic solution method employed in *UDEC* allows multiple local stability surfaces to be identified in one *UDEC* simulation. When using the **block factor-of-safety** command, model instability is detected by monitoring the unbalanced force ratio throughout the model. This provides a minimum global factor-of-safety for the model. In an alternative technique, presented here, material strengths are reduced in increments by a strength reduction factor. Unstable states for the model are identified at the global minimum state and then beyond that state. Unstable states of the model are identified at each stage as an assembly of gridpoints and contacts with velocities above a specified average value. The current strength reduction factor is assigned to unstable gridpoints and contacts for later contouring.

If the strength is reduced in small intervals, progressively more regions of gridpoints and contacts can be identified as unstable. By monitoring the velocities, it is possible to delineate the regions of unstable gridpoints and contacts by different strength factors and produce a plot of factor-of-safety contours. This plot can be used to locate multiple possible failure surfaces, and is comparable to the safety map developed using the limit equilibrium method.

This technique is demonstrated for a slope profile consisting of two double-inclination slopes separated by a horizontal berm. This example is taken from Cheng et al. (2007), who produced a set of local minimum stability states for this slope using the Morgenstern-Price limit equilibrium method. The slope configuration and resulting local minima locations are shown in '560F1016'.

UDEC Model

The *UDEC* data file created for this example is listed in Example 2.4 and Example 2.5. A *UDEC* simulation is first run to determine the global minimum factor of safety for this slope using the **block factory-of-safety** command. The result, shown by the shear strain contour plot in Figure 2.17, is a global minimum factor-of-safety of 1.29, with a failure surface that corresponds to the surface with smallest factor-of-safety value reported in Figure 2.16.

The safety factor from the **block factory-of-safety** command identifies the starting factor to develop a set of factor-of-safety contours for this model. Factor-of-safety contours are calculated for this slope model by using the **block solve fscontour** command. The command reduces the zone and contact Mohr-Coulomb strengths, cohesion and friction, incrementally. A stable or new unstable state is determined at each strength-reduction increment, and if the state is unstable, the portion of the model that is failing is identified by evaluating gridpoint and contact velocities. Gridpoints and contacts with velocities greater than a specified value are identified as failing, and are assigned the current strength-reduction increment factor, which is stored. After the simulation is completed for the selected range of strength-reduction increments, a contour plot of the stored values of the strength reduction factors is produced. This is a factor-of-safety contour plot.

The input values for the **block solve fscontour** command are the starting value for strength reduction, **minimum-factor**, the reduction factor increment, **factor-increment**, the maximum cycle limit for each stage, **maximum-cycles**, number of increments (stages), **total-stages**, and the limiting velocity threshold for a gridpoint at failure, **velocity-limit**.

The maximum cycle limit and velocity limit are problem-dependent; their values may be selected after trial runs with strength properties reduced to determine the velocity magnitude level at which failing gridpoints are well-defined. One of the ways to determine these quantities, is to use information from an already performed factor-of-safety analysis. In this example, the minimum factor of safety is found to be 1.29. Velocities of the gridpoints in the failed region are in the range (0.5 to 0.6) as shown in Figure 2.18. A total of 27,000 steps were taken to detect slope failure. (i.e., the number of steps taken during the **block factor-of-safety** calculation). These values are used as input parameters for the **block solve fscontour** command:

```
block solve fscontour minimum-factor 1.29, factor-increment 0.05, ...
  maximum-cycles 27000 velocity-limit 0.5 totoal-stages 6
```

The factor-of-safety contour plot produced for this example is shown in Figure 2.19. The contours compare quite well with the local minima surfaces plot in Figure 2.16. Note that the global minimum contour line (at a factor of 1.3) in Figure 2.16 closely matches the smallest local minimum surface in Figure 2.19. The next contour line, at factor of 1.35 below the berm, also compares well with the failure surfaces identified in Figure 2.16. The remainder of the factor-of-safety contours are slightly greater than contours in Figure 2.16).

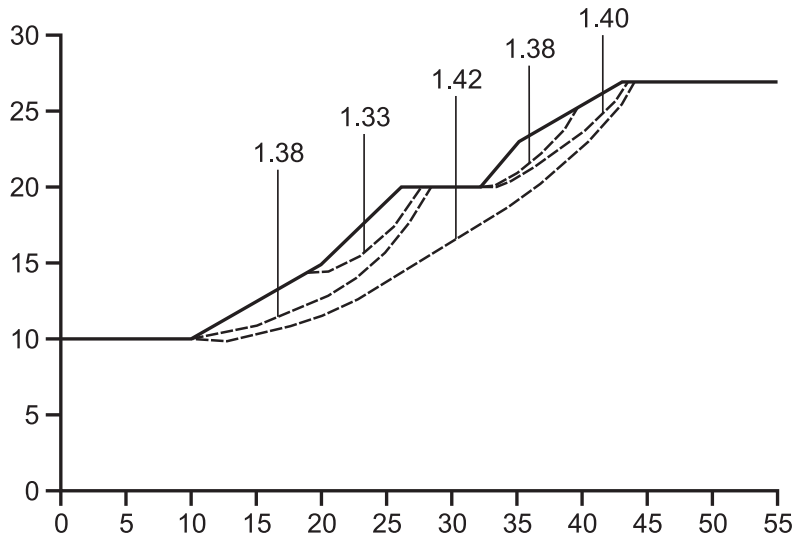

Figure 2.16 Local minima surfaces from limit equilibrium solution for slope with beam (from Cheng et al. 2007)

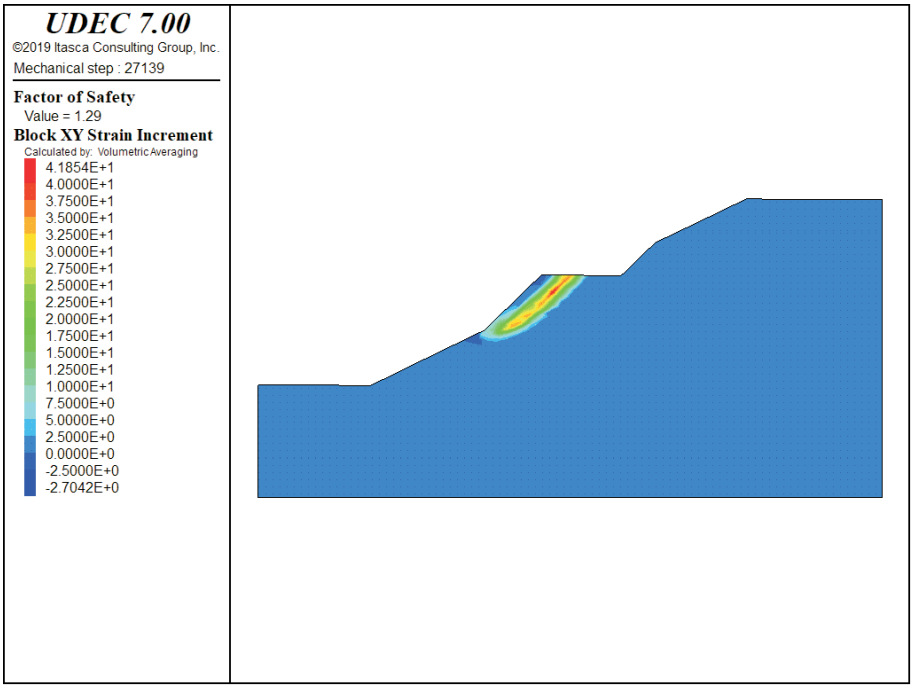

Figure 2.17 Failure surface for global FOS

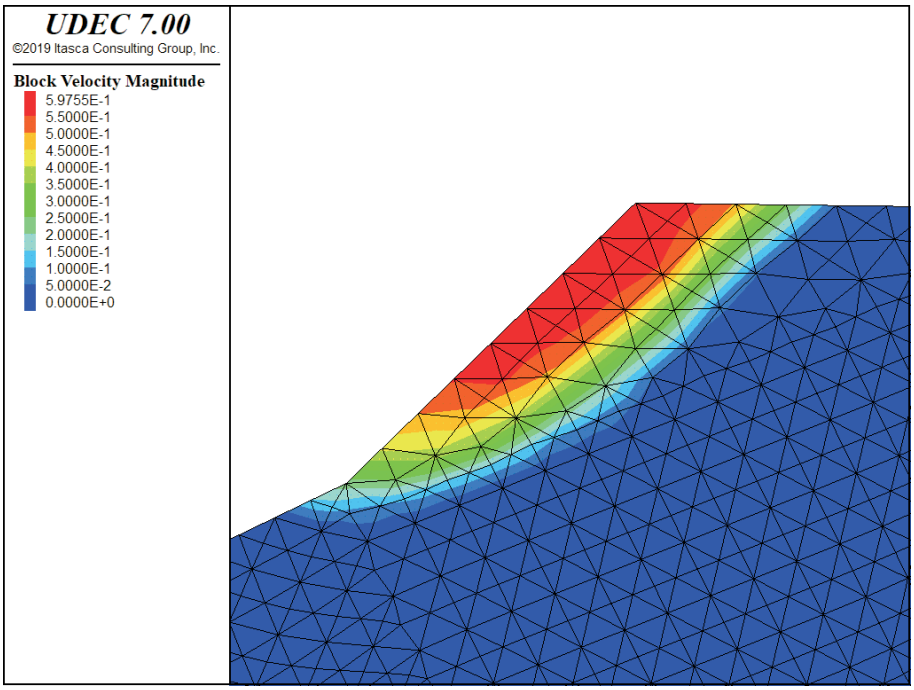

Figure 2.18 Gridpoint velocities at the onset of failure

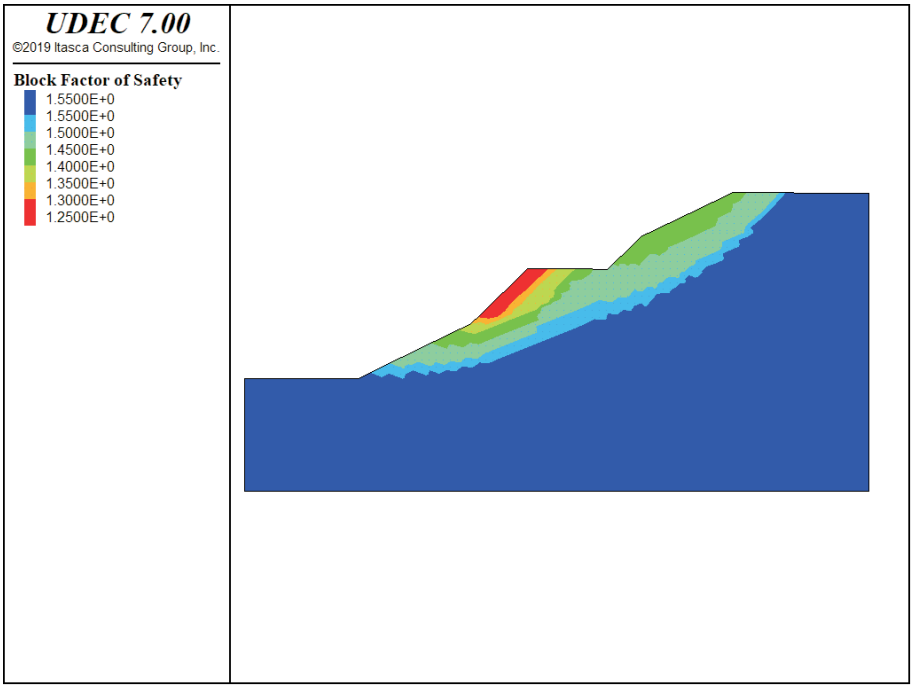

Figure 2.19 Factor of safety contour plot

In practice, several runs can be made with reduced strengths to evaluate velocities of the various regions at failure and a threshold value for the velocity magnitude and step number, as well as starting value for **block solve fscontour** calculations. In general, a range of values of input parameters can be found that produces identical factor-of-safety contour results.

This exercise demonstrates that the strength reduction method can be applied to produce multiple potential failure surfaces in one simulation by monitoring failure in terms of the development of unstable regions (defined by high gridpoint velocities) as the strength of the material is incrementally reduced. The method of selecting the input parameters based on the factor-of-safety calculation shows good correlation with the limit-equilibrium-method calculated values for the bench slope shown in Figure 2.15. If more accuracy is needed, further trial runs with reduced strength should be performed to evaluate in more detail velocity magnitude and step number at which failing points are well defined. It is best to have an actual failure case to calibrated the factor of safety contours for the insitu properties. Also it is a good idea to observe the failure mechanism in terms of strain and velocities to make cetain they make sense for a particlar case.

Example 2.4 Global factor-of-safety calculations for slope with berm

```
;fos.dat
;solve factor of safety example
model new
block tolerance corner-round-length .001
block create polygon ...
  0,0 0,10 10,10 20,15 25,20 32,20 35,23 43,27 55,27 55,0
block zone generate  edge 1
;
block zone cmodel assign mohr-coulomb density 2000 bulk 6.25e6 ...
  shear 2.885e6 cohesion 5000.0 friction 30.0 dilation 0.0 ...
  tension 1.0e10 flag-brittle off
;
block gridpoint apply vel-x 0 range pos-x 0.0
block gridpoint apply vel-x 0 range pos-x 55.0
block gridpoint apply vel-y 0 range pos-y 0.0
block gridpoint apply vel-x 0 range pos-y 0.0
;
block mechanical gravity 0 -10.0
block mechanical history unbalanced-maximum
block solve ratio 1e-6 elastic

model save 'Insitu'
model restore 'Insitu'
block gridpoint init velocity-x 0
block gridpoint init velocity-y 0
block gridpoint init displacement-x 0
block gridpoint init displacement-y 0
;
block factor-of-safety no-restore file 'fosmode_fos'
;
;
```

Example 2.5 Local factor-of-safety calculations for slope with berm

```
;fscont.dat
;factor of safety contour example
model restore 'Insitu'
block gridpoint init velocity-x 0
block gridpoint init velocity-y 0
block gridpoint init displacement-x 0
block gridpoint init displacement-y 0
;
```

```
block solve ratio 1e-5 fscont mini-factor 1.29 vel-limit .5 ...
  factor-inc 0.05 max-cyc 27000 tot-stage 6 ...
  file 'foscont_fscont';
;
```

2.6 References

Abramson, L. W., et al. ***Slope Stability and Stabilization Methods***, 2nd Ed. John Wiley & Sons, Inc. New York, USA (2002).

Baker, R., and D. Leshchinsky. "Spatial distribution of safety factors," *J. Geotech. Geoenviron. Eng.*, ***127***(2), 135-45 (2001).

Bishop, A. W. "The Use of the Slip Circle in the Stability Analysis of Earth Slopes," *Géotechnique*, ***5***, 7-17 (1955).

Chen, W.-F. ***Limit Analysis and Soil Plasticity***. J. Ross Publishing (2007).

Cheng, Y. M., T. Lansivaara and W. B. Wei. "Two-dimensional slope stability analysis by limit equilibrium and strength reduction methods," *Computers and Geotechnics*, ***34***, 137-150 (2007).

Chen, W.-F. ***Limit Analysis and Soil Plasticity***. J. Ross Publishing (2007).

Davis, R. O., and A. P. S. Selvadurai. ***Plasticity and Geomechanics***. Cambridge University Press (2002).

Dawson, E. M., and W. H. Roth. "Slope Stability Analysis with FLAC," in ***FLAC and Numerical Modeling in Geomechanics (Proceedings of the International FLAC Symposium on Numerical Modeling in Geomechanics, Minneapolis, Minnesota, September 1999)***, pp. 3-9. C. Detournay and R. Hart, eds. Rotterdam: A. A. Balkema (1999).

Dawson, E. M., W. H. Roth and A. Drescher. "Slope Stability Analysis by Strength Reduction," *Géotechnique*, ***49***(6), 835-840 (1999).

Dawson, E., K. You and Y. Park. "Strength-Reduction Stability Analysis of Rock Slopes Using the Hoek-Brown Failure Criterion," in ***Trends in Rock Mechanics (Proceedings of Sessions of Geo-Denver 2000, Denver, Colorado, August 2000)***. Geotechnical Special Publication No. 102, pp. 65-77. J. F. Labuz, S. D. Glaser and E. Dawson, eds. Reston, Virginia: ASCE (2000).

Donald, I. B., and S. K. Giam. "Application of the nodal displacement method to slope stability analysis," in ***Proceedings of the 5th Australia-New Zealand Conference on Geomechanics (Sydney, Australia, August 1988)***, pp. 456-460. Sydney: Institution of Engineers (1988).

Drescher, A., and E. Detournay. "Limit load in transitional failure mechanisms for associative and non-associative materials," *Géotechnique*, ***43***, 443-456 (1993).

Fellenius, W. "Calculation of the stability of earth dams," ***Proceedings of the 2nd Congress on Large Dams (Washington D. C.)***, Vol. 4. U. S. Government Printing Office (1936).

Fredlund, D. G., and J. Krahn. "Comparison of Slope Stability Methods of Analysis," *Can. Geotech. J.*, ***14***, 429-439 (1977).

Fu, W., and Y. Liao. "Non-linear shear strength reduction technique in slope stability calculation," *Computers and Geotechnics*, ***37***, 288-298 (2009).

Griffiths, D. V., and P. A. Lane. "Slope Stability Analysis by Finite Elements," *Géotechnique*, ***49***(3), 387-403 (1999).

Hammah, R. E., et al. "The shear strength reduction method for the generalized Hoek-Brown criterion," ARMA/USRMS 05-810 (2005).

Hoek, E., C. Carranza-Torres and B. Corkum. "Hoek-Brown Failure Criterion – 2002 Edition," in ***Proceedings of NARMS-TAC 2002, 5th North American Rock Mechanics Symposium and 17th Tunnelling Association of Canada Conference – Toronto, Canada – July 7 to 10, 2002***. Vol. 1., pp. 267-271. R. Hammah, et al., eds. Toronto: University of Toronto Press, 2002.

Janbu, N. "Slope stability computations," in ***Soil Mech. and Found. Engrg. Rep.***, The Technical University of Norway, Trondheim, Norway (1968).

Li, A. J., R. S. Merifield and A. V. Lyamin. "Stability charts for rock slopes based on the Hoek-Brown failure criterion," *Int. J. Rock Mech. and Mining Sci.*, ***45***, 689-700 (2008).

Lorig, L., and P. Varona. "Numerical Analysis," in ***Rock Slope Engineering***, pp. 218-244. D. C. Wyllie and C. W. Mah, eds. London: Spon Press (2004).

Lowe, J., and L. Karafiath. "Stability of Earth Dams upon Drawdown," in ***Proceedings of the 1st Pan-Am. Conference on Soil Mechanics and Foundation Engineering (Mexico City, Mexico)***, Vol. 2, pp. 537-552 (1960).

Matsui, T., and K. C. San. "Finite element slope stability analysis by shear strength reduction technique," *Soils and Foundations*, ***32*** (1) 59-70 (1992).

Michalowski, R. "Stability Charts for Uniform Slopes," *J. Geotech. Geoenviron. Eng.*, ***128***(4), 351-355 (April 2002).

Morgenstern, N. R., and V. E. Price. "The analysis of the stability of general slip surfaces," *Géotechnique*, ***15***(1), 79-93 (1965).

Naylor, D. J. "Finite elements and slope stability," in ***Numerical Methods in Geomechanics (Proceedings of the NATO Advanced Study Institute, Lisbon, Portugal)***, pp. 229-244. J. B. Martins, ed. D. Reidel Publishing Company (1982).

Shukha, R., and R. Baker. "Mesh geometry effects on slope stability calculation by FLAC strength reduction method – linear and non-linear criteria," in ***FLAC and Numerical Modeling in Geomechanics – 2003 (Proceedings of the 3rd International FLAC Symposium on Numerical Modeling in Geomechanics, Sudbury, Ontario, Canada, October 2003)***, pp. 109-116. R. Brummer et al., eds. Lisse: A. A. Balkema (2003).

Spencer, E. "A method of analysis of the stability of embankments assuming parallel interslice forces," *Géotechnique*, ***17***(1), 11-26 (1967).

Taylor, D. W. "Stability of earth slopes," *J. Boston Soc. Civ. Eng.*, ***24***, 197-246 (1937).

Transportation Research Board. "Landslides: Investigation and Mitigation," ***TRB Special Report 247***, National Academy Press, Washington D.C. (1996).

Ugai, K. "A method of calculation of total factor of safety of slopes by elasto-plastic FEM," *Soils and Foundations*, ***29*** (2) 190-195, (in Japanese) 1989.

Ugai, K., and D. Leshchinsky. "Three-dimensional limit equilibrium and finite element analyses: a comparison of results," *Soils and Foundations*, ***35*** (4) 1-7 (1995).

Wenxi, Fu, and Yi Liao. "Non-linear shear strength reduction technique in slope stability calculation," *Computers and Geotechnics*, ***37***, 288-298 (2010).

Zienkiewicz, O. C., C. Humpheson and R. W. Lewis. "Associated and non-associated visco-plasticity and plasticity in soil mechanics," *Géotechnique*, ***25***(4), 671-689 (1975).